

Article

Hybrid PV/T Heat Pump System with PCM for Combined Heating, Cooling and Power Provision in Buildings

K. B. Prakash¹, Mohammed Almeshaal², Manoj Kumar Pasupathi^{3,*}, Subramaniyan Chinnasamy¹, S. Saravanakumar⁴ and S. Rajesh Ruban⁵

- ¹ Department of Mechanical Engineering, Bannari Amman Institute of Technology, Sathyamangalam, Erode 638401, Tamil Nadu, India; prakashkb@bitsathy.ac.in (K.B.P.)
- ² Department of Mechanical and Industrial Engineering, College of Engineering, Imam Mohammad Ibn Saud Islamic University, Riyadh 11432, Saudi Arabia
- ³ Department of Mechanical Engineering, KPR Institute of Engineering and Technology, Coimbatore 641407, Tamil Nadu, India
- ⁴ Department of Mechanical Engineering, M.Kumarasamy College of Engineering, Karur 639113, Tamil Nadu, India
- ⁵ Department of Mechanical Engineering, Karunya Institute of Technology and Sciences, Coimbatore 641114, Tamil Nadu, India
- * Correspondence: manojkumar.p@kpriet.ac.in

Abstract: Hybrid photovoltaic-thermal heat pump (PV/T-HP) solar energy systems are promising since they can achieve a system total efficiency greater than 80%. By maximizing the output of a PV/T system for simultaneous heating and cooling, this strategy can meet over 60% of urban households' heating needs and around 40% of their cooling needs. In this work, a novel PV/T evaporator was designed, fabricated, and an aluminium foil encapsulated hydrated salt (HS36) PCM was integrated with the PV/T evaporator of the PV/T direct expansion heat pump system (PV/T-DXHP). Energy analysis was carried out on the PV/T-DXHP system with PCM in tropical climate regions of India for achieving net zero energy buildings. The experimental study revealed that the average PV electricity efficiency was 14.17%, which is near the PV panel's STC value. The average thermal efficiency of the system was 104.38%, and the PV/T system's average overall efficiency was 117.58%. The heating and cooling COPs of the system were 5.73 and 4.62, respectively. It was concluded that net-zero energy buildings are possible with the help of photovoltaic heat pump systems that use PCM and solar energy to make electricity, cool spaces, and heat water.

Keywords: solar photovoltaic; heat pump; phase change materials; COP; energy



Citation: Prakash, K.B.; Almeshaal, M.; Pasupathi, M.K.; Chinnasamy, S.; Saravanakumar, S.; Rajesh Ruban, S. Hybrid PV/T Heat Pump System with PCM for Combined Heating, Cooling and Power Provision in Buildings. *Buildings* **2023**, *13*, 1133. <https://doi.org/10.3390/buildings13051133>

Academic Editor: Xi Chen

Received: 18 March 2023

Revised: 18 April 2023

Accepted: 20 April 2023

Published: 24 April 2023



Copyright: © 2023 by the authors. Licensee MDPI, Basel, Switzerland. This article is an open access article distributed under the terms and conditions of the Creative Commons Attribution (CC BY) license (<https://creativecommons.org/licenses/by/4.0/>).

1. Introduction

Nowadays, most people are aware of the impact of carbon emissions on the environment and the need to reduce the use of fossil fuels to keep the world average temperature rise to less than 2 °C in recent decades [1]. The world's energy system has to be changed to a more sustainable one to reduce carbon emissions and global temperature rise [2]. The heating and cooling devices consume the most considerable energy in India, accounting for 51% of all final energy consumption. Cooling of spaces (52%), processes (30%), and water (10%) account for the majority of demand, with space heating demand still being moderate but rapidly increasing. A total of 45% of energy use is in heating and cooling buildings in the residential sector, followed by industry with 37% and services with 18% [3]. Reducing the use of fossil fuels, lowering carbon emissions, and increasing the use of sustainable sources of energy, is crucial to continue developing and placing renewable building technology into use. Affordably deploying solar energy was generally recognized as a significant worldwide engineering problem because of its potential to significantly impact the reduction of our dependency on fossil fuels and the integration of renewable energy

sources into the building environment. Solar power generating and solar water heating systems are advantageous since they may provide both water heating and electricity, which stand out as possible decarbonization approaches [3]. There are a few drawbacks to solar water heating (SWH) systems that could prevent them from being widely used. The SWH water heating system is dependent on sunlight, and it generates a limited hot water supply [4]. Similarly, PV panels have lower efficiency limitations due to the rise in PV module temperature [5]. Cooling spaces with air conditioner (AC) systems are commonplace in modern buildings, especially in congested urban regions. Air conditioning in buildings is in high demand due to rising temperatures and expanding metropolitan areas in India. While HVAC systems are becoming increasingly common in wealthy nations, India needs to catch up due to several barriers to entry. AC systems also cost a lot to run and maintain because they use a lot of energy [6]. Hence, the technologies used to produce hot water, electricity, and space cooling have limitations, and combining them into a single system can enhance its performance. Hybrid photovoltaic-thermal heat pump (PV/T-HP) solar energy systems look good and can solve the problems discussed since they can achieve a system total efficiency greater than 80%. By maximizing the output of a PV/T system for simultaneous electricity generation, heating, and cooling, this strategy can meet over 60% of urban households' heating needs and around 40% of their cooling needs.

All buildings require the capacity to independently produce electricity that can conserve energy and utilize the heat generated for space cooling and water heating. Hence, Fischer and Madani [7], who also looked at this, considered combining solar PV with heat pumps a highly successful technique to achieve more electricity savings. Similar findings from Khouya's investigations [8] have shown that focused PV/T and heat pumps may significantly lower electrical energy usage. Also, the most important thing the authors found was that hybrid systems based on renewable energy could provide electricity at a reasonable price [9]. Adding heat pumps with PV/T as a hybrid component was researched to increase the system's overall energy efficiency. Kamel et al. [10] placed a particular emphasis on this idea in the research that they conducted on the possibility of hybrid systems undergoing evolution and improvement. Heat pumps can theoretically give the power system more flexibility if the appropriate design technique was applied. Cascade heat pumps can often produce cooling water in addition to hot water at medium and high temperatures, making them useful for various applications [11], including drying and cooling buildings. Yaolin Lin and colleagues [12] researched a variety of PV/T-HP systems and found that the efficiency of photoelectric and photothermal conversions has significantly improved. The photovoltaic cell's operating temperature can be lowered, which is a bonus, while photoelectric efficiency may be improved. The PV/T heat-collection module works as the heat source for the heat pump. This causes an increase in the evaporation temperature and the evaporation pressure of the evaporator's working fluid, which raises the heat pump's coefficient of performance. Kong et al. [13] undertook a numerical analysis of the PV/T-based hybrid system for space cooling, heating, and PV panel cooling. They found that the system had a coefficient of performance COP of 4.5 and that the temperature drop in the panel was between 5 and 15 degrees Celsius. Experiments by Besagni et al. [14] on the hybrid PVT system revealed a COP of 4.2 on average and a temperature drop of 10–20 degrees Celsius in the PV panel. The heat pump PV/T system was examined by Shao et al. [15], and the researchers found that it had a maximum COP of 4.8 and a module efficiency of 12%. The heat pump PV/T system's coefficient of performance (COP) was determined to be 3.7 on average by Hong Li Yue Sun et al. [16]. Zhou et al. [17] carried out the experimental study on the HP PV/T system and found that it had a COP of 4.7, was 13.1% efficient in generating electricity, and 56.6% efficient in extracting heat. Min Yu et al. [18] examined the potential of a micro-channel loop PV/T HP system and discovered that by using R410a as the refrigerant, they could increase efficiency by 18.55%. The researchers found that by using R410a as the refrigerant, they achieved an increase in efficiency of 18.55%. Zhiying Song and colleagues [19] researched the PV/T heat pump system, which had a maximum COP of 5.45 and provided the highest possible level of

electrical efficiency of 11.66%. Emmanuel et al. [20] performed a numerical investigation of the PV/T HP system and discovered that the temperature of the PV/T was reduced to a maximum of 17.16 °C. Sajidabbas et al. [21] conducted tests on the PV/T HP system and found that its efficiency increased by 14.08% and that its average coefficient of performance was 6.11. A few researchers used PCMs below the panel of the PV/T system to regulate the thermal energy and boost the electrical performance by lowering the temperatures of the PV cells [22–24]. Many researchers used high [25,26] as well as low thermal conductivity PCMs [27], and metal foam-coupled PCM [28]. However, most of the research works focused on an indirect expansion heat pump for building space heating, PV cooling, and electricity.

On the other hand, most of the information from earlier research was based on indirect expansion HP for a cold environment. Only a few researchers conducted the experimental performance analysis of a hybrid PV/T-DXHP system. However, the studies focused on something other than PCM-integrated PV/T evaporators in PV/T-DXHP systems for generating electricity, PV cooling, space heating, and hot water in hot climatic regions. The novelty of this work was integrating a new novel butterfly serpentine flow (BSF) collector as a PV/T evaporator and hydrated salt (HS 36, an aluminium foil encapsulated PCM) to enhance the performance of the PV/T-DXHP system and to meet the building requirements. The objective of this work is to suggest a suitable hybrid alternative instead of using different systems for space cooling, water heating, and power generation in buildings. A combined approach is used for space cooling, water heating, and PV power generation in buildings. Hence, a hybrid PV/T-DXHP direct expansion HP system with phase change material (PCM) has been proposed in this study to provide a building's needs, i.e., electricity, space cooling, PV cooling, and hot water. This research was conducted to find ways for homes and businesses to use energy more efficiently. It was accomplished by developing a hybrid system that addresses the issues identified with photovoltaic panels and HVAC systems. Energy analysis was carried out on the PV/T DXHP system with BSF pattern profile coil and hydrated salt PCM (HS36) at the PV/T evaporator side for PV panel cooling, space cooling, water heating, and electricity generation applications. In this work, the electrical conversion efficiency (η_{el}), thermal efficiency (η_{th}), COP_{HP} , and $COP_{overall}$ of the PV/T-DXHP-PCM system were analyzed and compared with those of a reference uncooled PV system.

2. System Description

A PV/T-DXHP-PCM system was designed and fabricated for hot Indian climatic conditions. This country's climate was generally hot and humid all year. It receives a lot of sunlight due to its geographical position and solid solar radiation, averaging 20.04–26.01 MJ/m² per day and an annual total of around 5703 MJ/m². Compared to the other months of the year, summertime has a larger daily solar energy average than the other times of the year. The average temperature of the surrounding air on any day during the year was 31 °C. Because there is abundant yearly solar energy and a heat supply from the surrounding environment. Any time of day or year can heat water with the PV/T-DXHP-PCM because of its adaptability and versatility. A novel, new butterfly serpentine flow profile was developed and used as a PV/T-PCM evaporator with a heat pump setup. The detailed description of the experimental design was explained in detail in subsequent subsections.

2.1. PV/T Collector Design

The serpentine flow pattern used in this work was shaped like a butterfly structure; as a result, it is known as the Butterfly Serpentine Flow (BSF) Pattern. Because the center of the PV panel encounters higher temperatures than the bottom and top areas. Hence, the BSF flow pattern was created and chosen to cool the PV's center part effectively. Figure 1 shows the pattern of PV/T collector's intricate design. Figure 2 shows the extended views of the PV/T-PCM evaporator used in this work. The fabrication process for the PV/T

collector/evaporator is shown in Figure 3. The PV/T evaporator combines heat from a collector and electricity from PV panels (BSFC pattern copper coil). A 260 W polycrystalline photovoltaic (PV) panel and a 60-cell PV (p-Si) module were used to create the PV/T evaporator. Table 1 provides technical information about PV panels. The chosen location’s average outdoor air temperature (T_a) is 31 °C. More heat was transferred from the PCM to the aluminium plate when the PCM’s melting point was between T_a+3 °C and T_a+6 °C [29], due to better heat dissipation. Hence, the PCM used for this work was hydrated salt (HS36), which has a 36 °C melting point. The PCM was encapsulated in aluminium foil packets, which were thin and effective at transferring heat. An aluminium foil of 30 cm width, 57 cm height, and 3 mm thick encases the HS36 salt-hydrate PCM. Using Equation (1), it was determined the PCM’s mass [29] was 9 kg. Underneath the PV/T evaporator, there were nine packets of HS36, each having 1 kg., as shown in Figure 3. Table 2 displays the technical parameters of PCM.

$$m_{PCM} = \frac{Q_{ch}}{Q_{LH-pcm} + \int_i^m C_{ps}(T)dT + \int_m^f C_{pl}(T)dT} \tag{1}$$

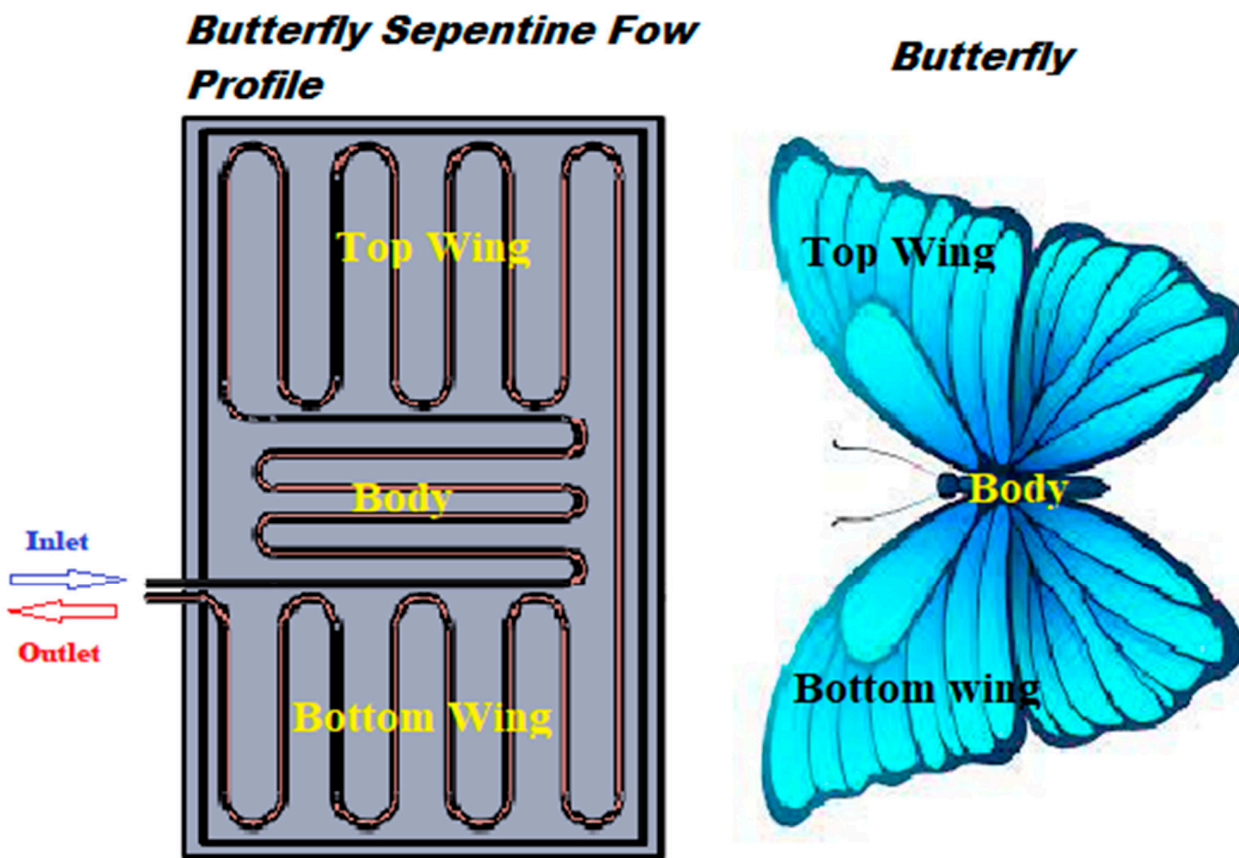


Figure 1. Schematic view of Butterfly serpentine flow profile (BSFP).

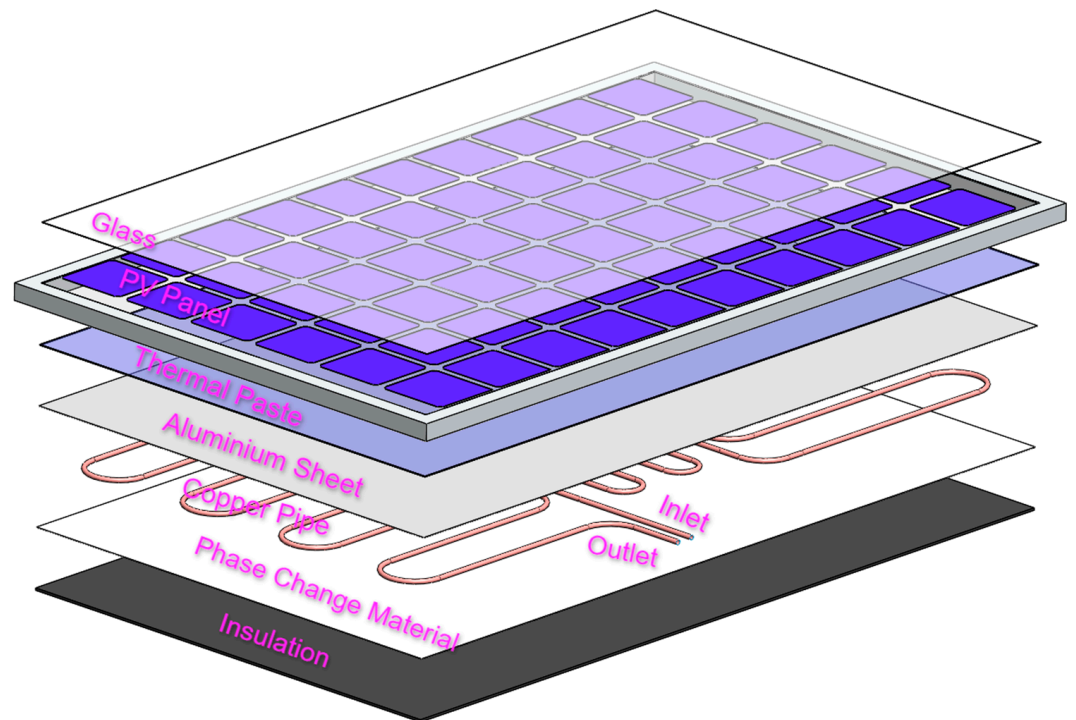


Figure 2. Layers of the PV-PCM system.

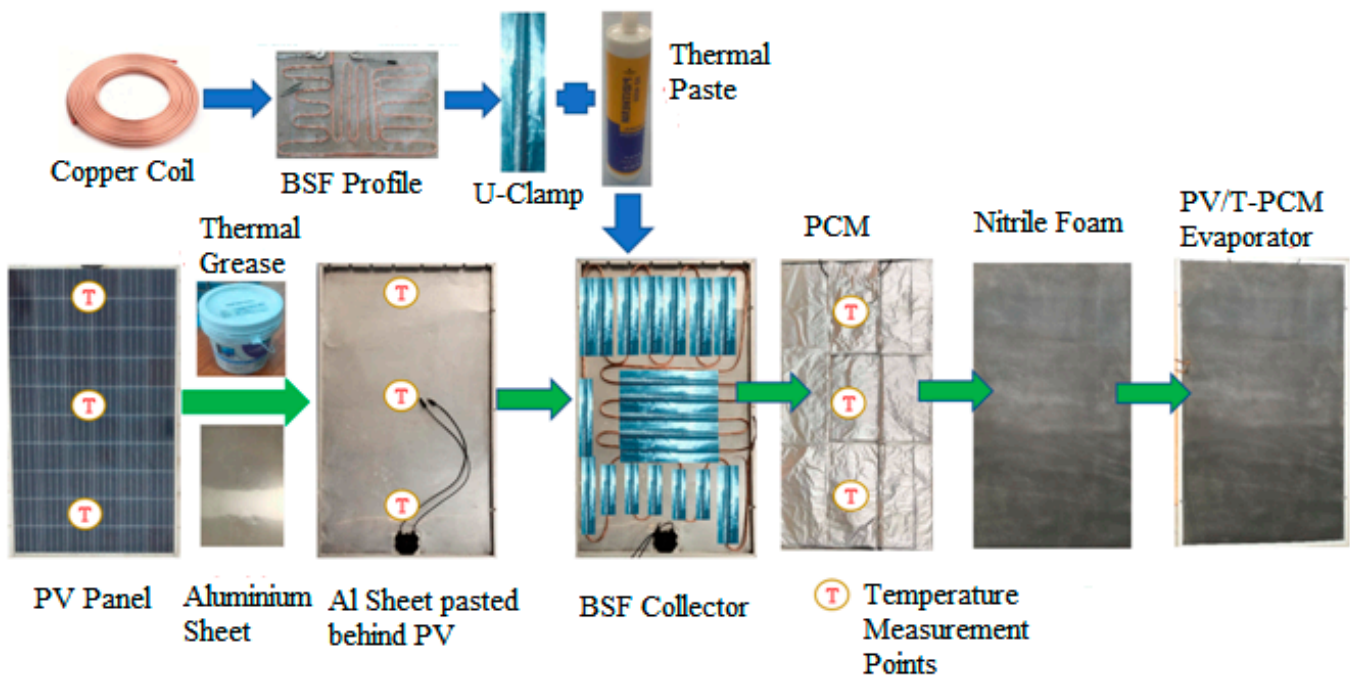


Figure 3. Methodology of PV/T PCM evaporator fabrication.

Table 1. Specification of PV.

Parameters	Range
P_{\max}	260 W
$V_{\text{mp at } P_{\max}}$	31.0 V
$I_{\text{mp at } P_{\max}}$	8.38 A
V_{oc}	38.4 V
I_{sc}	8.92 A
Size of PV	1661 × 991 × 35 mm
Mass of PV	18 kgs

Table 2. PCM—salt hydrate (HS36) Properties.

Parameters	Range
T_m	36.0 °C
T_f	35.0 °C
Q_{LH}	166 kJ/kg
ρ_l	1850 kg/m ³
ρ_s	1967 kg/m ³
C_{pl}	2.32 kJ/kgK
C_{ps}	1.98 kJ/kgK
K_l	0.47 W/mK
K_s	0.5 W/mK

2.2. Experimental Setup

The schematic layout of the hybrid PV/T-DXHP-PCM system used in the study is shown in Figure 4, and Table 3 lists its characteristics. Sathyamangalam, Tamil Nadu, India, at latitude 11.5034° N and longitude 77.2444° E, is the location of the experimental setup. Experimental tests were performed on instances from 20 May to 30 May 2022. The latitude of the research site, which determines test apparatus inclination, was (β) 11.5° [30]. Figure 4 shows the steps for how the PV/T-DXHP-PCM experimental setup works in each of its many iterations. First, the refrigerant enters the PV/T evaporator and air source evaporator (ASE), which gain heat from solar energy and room air. Consequently, the R410A refrigerant vaporized in the evaporator, and a rotary hermetic compressor compressed the low-pressure vapour refrigerant that came from the evaporator. The high-pressure, high-temperature refrigerant vapour condenses and turns into a liquid as it flows through the condenser tubes inside the hot water storage tanks. During the throttling process, a high-pressure and high-temperature liquid refrigerant entered the capillary tube and was driven down to lower its pressure and temperature. The low-pressure and low-temperature liquid was consecutively passed through the evaporator and cycled continuously. To cut down on the amount of heat lost from the system into the surrounding air, thermal insulation was placed on top of the refrigerant tube circuit and storage tank of a heat pump. In this work, refrigerant was supplied to ASE continuously. However, for the PV/T evaporator, R410A was provided until the PCM temperature reached 38 °C and stopped when it reached 30 °C. The thermal performance of the PV/T-DXHP-PCM system depended on the kind of heat source being used. As a result, it is vital to examine the thermal and electrical characteristics of PV/T-DXHP-PCM to the ambient circumstances for applications involving electricity generation, water heating, the cooling of space, and the cooling of PV.

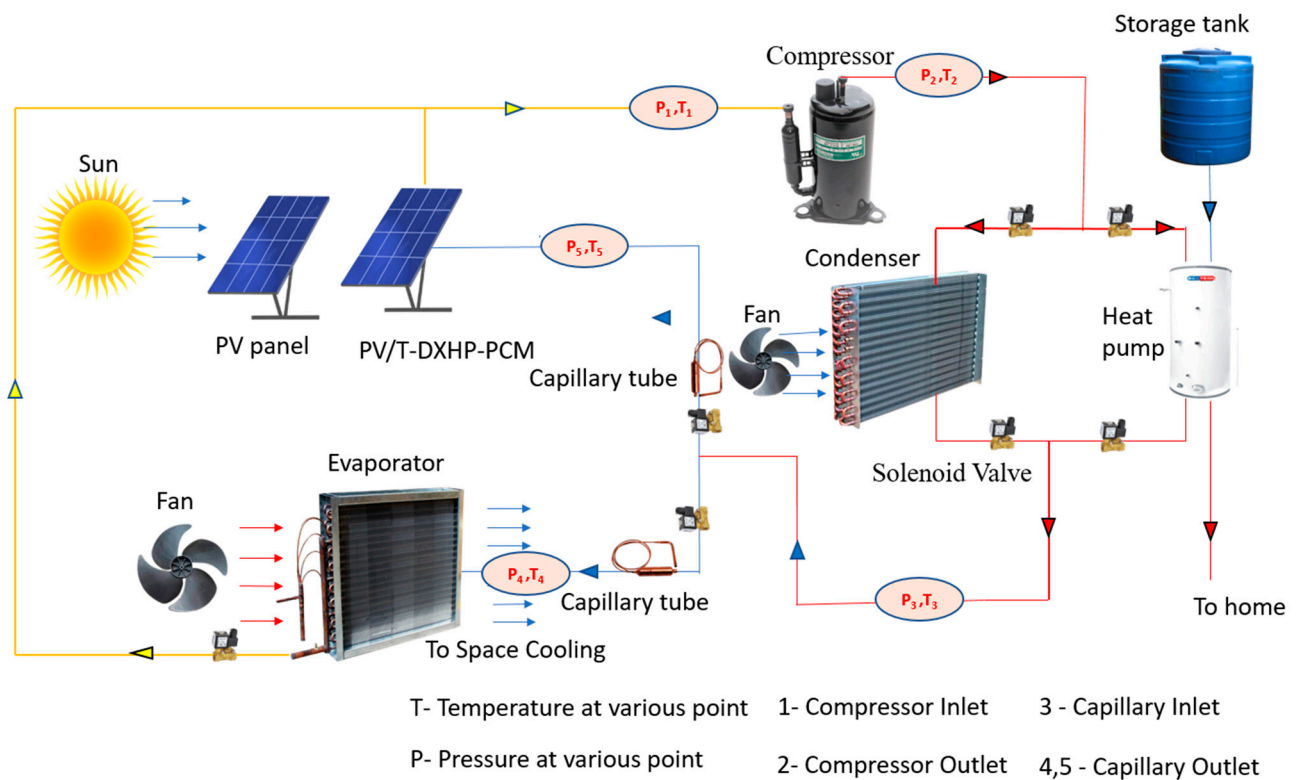


Figure 4. Schematic diagram of PV/T-DXHP-PCM system for water heating, space cooling and PV cooling.

Table 3. HP specification.

Components	Parameters	Value
Compressor	V_d	10.9 (cc/rev)
	CC	3500 W
	E_{Rp}	910 W
	I_R	4.1 A
	R	R410A
Condenser	Con_{od}	9.5 mm
	Con_{id}	7.7 mm
	V	600 L
Capillary tube	CT_{id}	1.5 mm
	CTI	500 mm

2.3. Measuring Devices

The Davis Wireless Vantage Pro-2 weather station recorded accurate, real-time readings of wind speed, dew point, relative humidity, and solar radiation. Pressure transmitters and thermocouples (PT-100) were utilized to monitor the R410A refrigerant's intake, output pressure, and temperatures throughout the system. An energy meter with a current sensor measures the compressor's electrical power consumption and instantaneous current use. The system's flow rate was monitored using a volumetric flow meter, and the electricity produced by the solar PV system was measured using a PV analyzer. A high-precision AIS-PPI UniLog Pro universal input data recorder system was used to link all the sensors. The measured parameters were sent to the computer with a 30-s interpolation period. Finally, the suggested hybrid system was assessed utilizing the results acquired from all of this measurement equipment, which included the thermal and electrical efficiency, COP.

2.4. Thermodynamic Analysis

The input energy of a PV system determines the output energy ratio (solar radiation on the photovoltaic surface). The conversion efficiency and the thermal efficiency η_{th} of a 260 W PV panel were found by Equations (2)–(4) [31].

$$\eta_{PVT} = \eta_{th} + \eta_{PV} \quad (2)$$

$$\eta_{el} = \frac{P_{max}}{A \times G} \quad (3)$$

$$\eta_{th} = \frac{Q_u}{A \times G} \quad (4)$$

Equation (5) is used to figure out how much useful heat was collected (Q_u) from the system [32].

$$Q_{uPV/T} = m_r(h_{out} - h_{in}) \quad (5)$$

The compressor's energy consumption [33], ref. [34] is shown in Equation (6).

$$P_{com} = m_r(h_{dis} - h_{suc}) / \eta_{iso} \quad (6)$$

Equation (7) represents the total heat supplied to the condenser [35].

$$Q_{cond} = m_r(h_{Con,out} - h_{Con,in}) = m_w C_{pw} (T_f - T_i) \quad (7)$$

Equation (8) shows how much heat takes from the space cooling by the evaporator.

$$Q_{eva,air} = m_r(h_{eva,in} - h_{eva,out}) \quad (8)$$

For a PV/T heat pump system, the COP (heating, cooling (CL), overall) was determined using Equations (9)–(11) [33]. Equation (12) is used to determine the PV/T-DXHP-PCM system's thermal efficiency (η_{thHP}) [34].

$$COP_{HP} = \frac{Q_{cond}}{P_{com}} \quad (9)$$

$$COP_{CL} = \frac{Q_{eva}}{P_{com}} \quad (10)$$

$$COP_{overall} = \frac{\Delta P_{max} + Q_{cond} + Q_{eva}}{P_{com}} \quad (11)$$

$$\eta_{thHP} = \frac{Q_{cond} - P_{com}}{A \times G} \quad (12)$$

2.5. Analysis of Uncertainty

There is a dearth of precise knowledge regarding the precision of the data presented in experimental investigations. As a result, an analysis of the devices uncertainty were performed to identify that the information utilized in the experimental testing was accurate. The error calculated was 3.2% for electrical efficiency, 4.1% for thermal efficiency, and 3.82% for temperatures. It was computed by utilising the Equation (13) [36]. The detailed errors of sensors are given in Table 4.

$$W_R = \left[\left(\frac{\partial R}{\partial x_1} W_1 \right)^2 + \left(\frac{\partial R}{\partial x_2} W_2 \right)^2 + \dots + \left(\frac{\partial R}{\partial x_n} W_n \right)^2 \right]^{1/2} \quad (13)$$

Table 4. Details of sensors used.

Instruments	Parameters	Range	Accuracy
Solar Station (Vantage Pro 2)	G	0–2000 W/m ²	±5%
DAQ (PPI)	-	16 UDI	±3%
PV Analyser	P _{max}	0–50 V and 0–20 A	±5%
K type Sensor	T _w , T _a , T _{pv}	0–1000 °C	±0.5
PT 100 (RTD)	T _r	(−100)–(+200) °C	±0.1
Pressure Transmitter	Pr	0–60 bar	±0.5
Current Sensor	I	0–10 A	±1%
Relative Humidity sensor	RH	0–100%	±3%

3. Result and Discussion

This section details the performance analysis of the hybrid PV/T-DXHP-PCM system from an energy point of view. The electrical and thermal efficiencies, and COP of a hybrid system were evaluated to assess its performance. Figure 5 depicts the graphical representations of the ambient conditions during the experimentation days. Experimentations were conducted from 20 May 2022 to 30 May 2022, and most of the days had similar ambient conditions and achieved identical performances. Hence, the PV/T-DXHP-PCM system's performance on 30 May 2022 was discussed in this work.

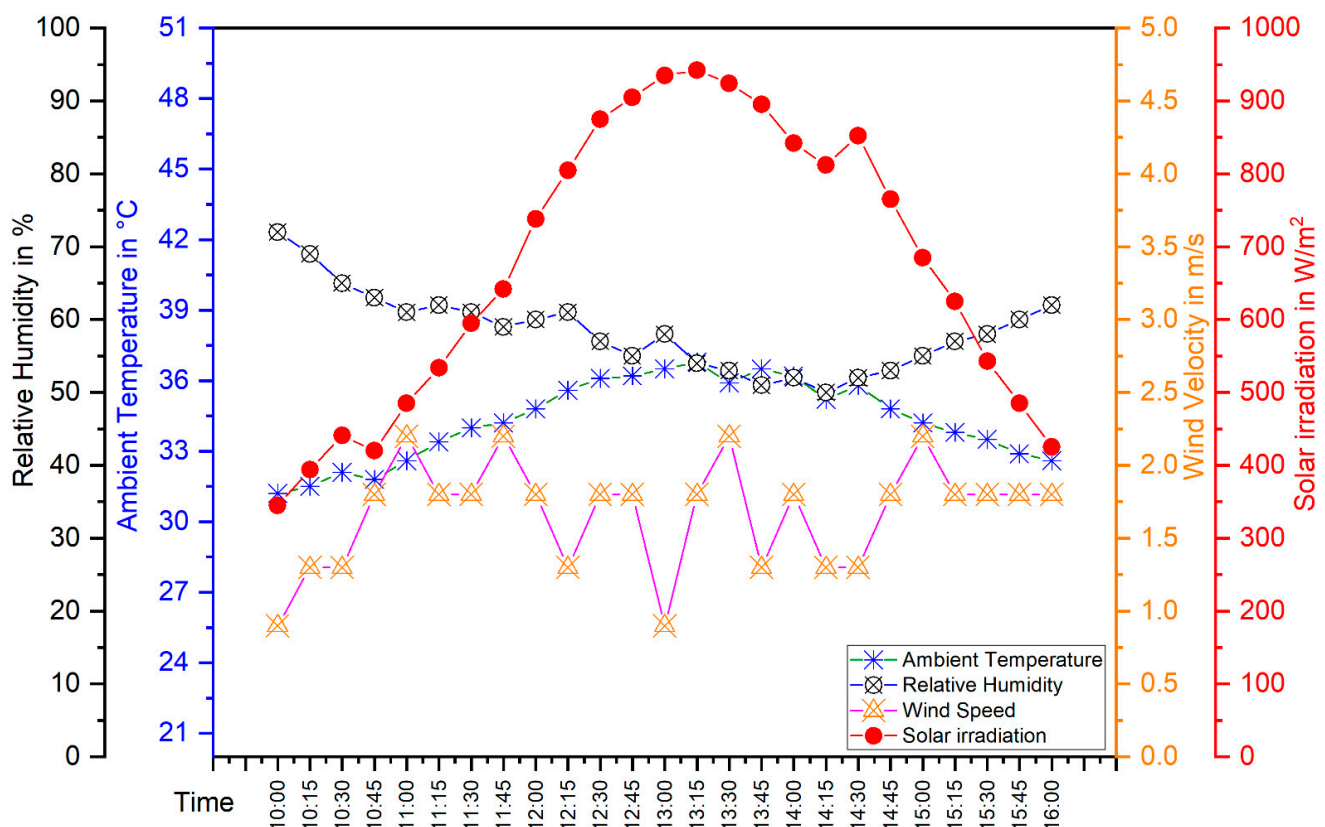


Figure 5. Variation in ambient temperature, solar irradiance, and wind speed on an hourly basis on 30 May 2022.

3.1. PV/T System's Dynamic Performance

The performance of the PV/T-DXHP-PCM system was assessed by simultaneously monitoring the electrical and thermal energy produced by the system. The overall system performance, including thermal and electrical components, was measured by efficiency and COP. Hourly changes in maximum PV power generation (P_{\max}) and electrical conversion efficiency (η_{el}) for the proposed and reference systems are shown in Figure 6. The difference between the two systems' electrical outputs at 942 W/m^2 was 43.30 W ; specifically, the proposed system generated 180.82 W , and the reference system generated 137.9 W . The electrical efficiency of this system peaked at 15.75% and dropped to 12.59% at its lowest point; the value of η_{el} varies by 4.73% between the proposed and reference systems. PV/T-DXHP-PCM and reference system generated an average P_{\max} of 142.53 W and 106.46 W , respectively. The Efficiency of the PV/T-DXHP system was higher than the regular PV system by a margin of at least 15% and as much as 72% . Electrically speaking, these two systems had respective averages of 14.17% and 9.56% regarding how efficiently they converted electricity. In addition, the standard test condition for the efficiency of photovoltaic modules is 16.5% , while the average electrical efficiency is 14.17% . This suggests that the method that has been proposed has increased the effectiveness of PV cells by optimizing solar energy outputs that are near the maximum power rating of the installed PV modules. By increasing sun irradiation by 100 W/m^2 , an extra 15.38 W of power can be generated. Similarly, a decline in cell temperature by one degree Celsius results in a 12.6 W gain in electrical output. Changes in electrical efficiency were 0.79% for every 100 W/m^2 of extra solar irradiation and 0.63% for every one degree Celsius drop in cell temperature. The sharp rise in electrical output from 400 W/m^2 to 1000 W/m^2 was easily seen in Figure 6. It has been shown that the proposed system's power output can be increased and the PV cells' temperature can be reduced by using a heat pump and a PCM.

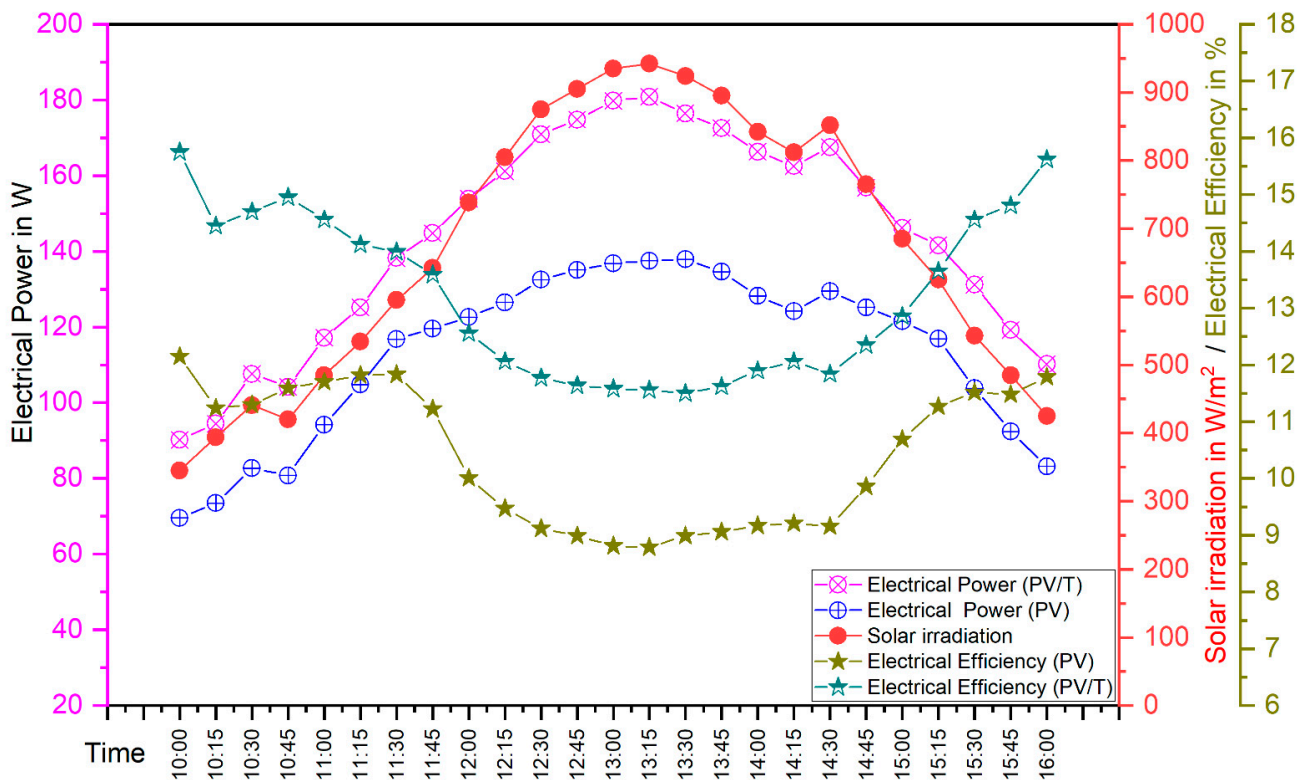


Figure 6. Hourly variation of electrical efficiency and electrical power.

Figure 7 presents the findings of the room temperature, the temperatures of the PV/T module, and the condenser water throughout the day. The temperature of the PV increased

in lockstep tandem with the temperature of the surrounding air (T_a), causing T_{PV} to rise. A PV cell's average temperature was calculated to be 34.59 °C and 65.59 °C for the PV/T-DXHP-PCM and the reference system, respectively. The PCM had a mean temperature of 33.52 °C. The most significant and most minor differences in ΔT_{PV} between the proposed and reference systems, respectively, were 40.3 °C and 21.3 °C. When contrasted with the reference system, it was discovered that the PV cell temperature of the proposed system was reduced by at least 40.68% and up to 52.11%. In general, the cold refrigerant generated by the heat pump can reduce the temperature of the PV module. As a result, the thermal collector output temperature can be kept lower than the T_{PV} of the proposed system. This is a significant factor in improving the efficiency of the PV/T system. The reference PV system had an average PV cell temperature that was 47.26% higher than the proposed system's average. The water temperature in the condenser rose by 2.83 °C and 2.63 °C for every change of 100 W/m² and 1 °C. When cold refrigerant was supplied to the PV/T-PCM evaporator, it was utilized to lower the temperature of the PV panel, which in turn increased the efficiency of the PV/T system. When this occurs, the average temperature difference between the refrigerant inlet (T_i) and output temperature (T_o) was between 3.58 and 22.96 °C. According to the findings of a field investigation conducted on the collectors, the system's thermal efficiency dropped when the temperature difference between T_o and T_i was less. The thermal absorber's outlet and intake temperatures directly influence the average thermal efficiency determined in this investigation, which was 104.38%. As a result of the increase in condenser temperature, the system's thermal efficiency continued to deteriorate as the amount of solar irradiation increased. The thermal efficiency was found to be high when the water temperature in the condenser was low, and vice versa. The overall efficiency of PV/T-DXHP-PCM was 117.58% on average, and the overall efficiency of the installed system as a whole decreased as the thermal efficiency decreased. As a result, it is clear that the overall efficiency of hybrid systems is more significant due to the PV/T, PCM, and heat pump systems' integration and that this integration produces positive results.

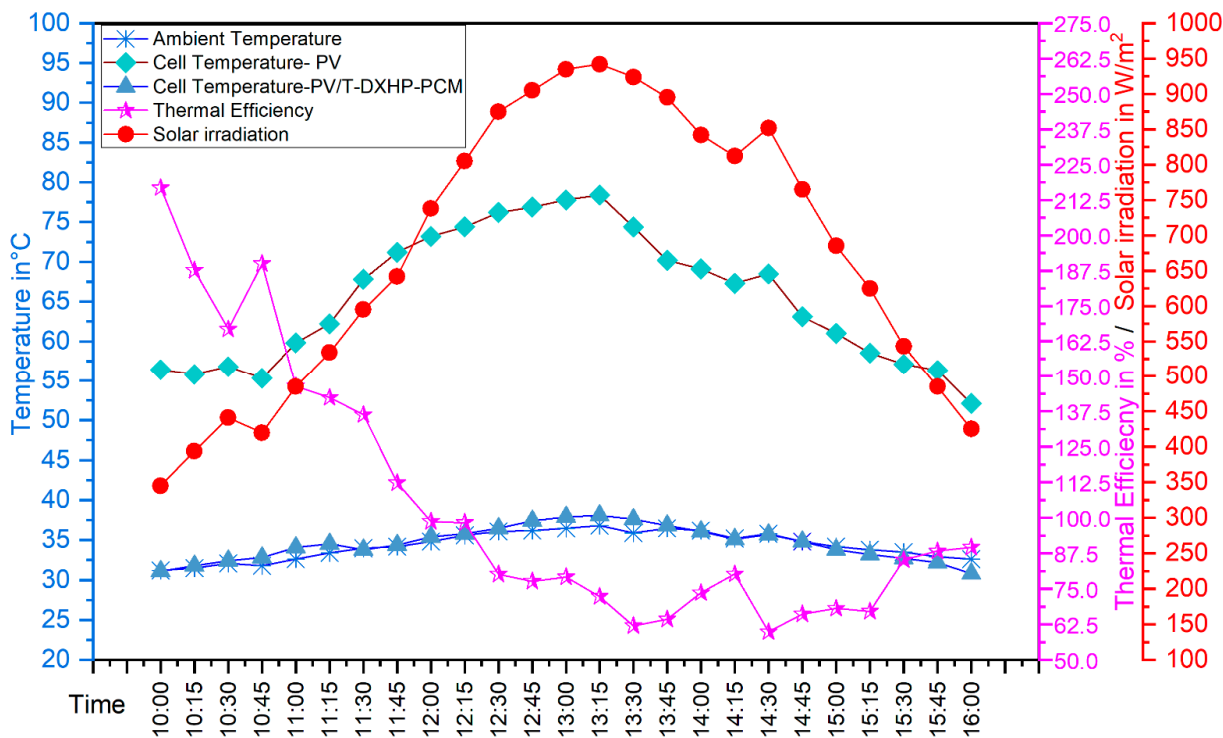


Figure 7. Hourly variation of T_{pv} , T_a , G , and η_{thHP} .

3.2. Dynamic Performance of the Hybrid PV/T-HP-PCM System Performance

This section summarizes the dynamic behaviour of the suggested PV/T-PCM evaporator and ASE system (Q_e), the condenser heat (Q_c), the COP, and the power consumption. Because of fluctuating levels of customer demand, the utilization of hot water could be more frequent. Therefore, a condensed tank with a capacity of 600 L and a maximum temperature of 60 °C was used to store the water. The hybrid heat pump system's performance was investigated, providing space cooling, PV cooling, hot water, and electricity generation between 10:00 and 14:00. The system was constructed so that the refrigerant flow into the PV/T evaporator is stopped when the PCM temperature hits 30 °C. It will begin again when the PCM temperature reaches 38 °C. Similarly, refrigerant flow into the air source evaporator starts when the temperature in the space reaches 26 °C and ceases when the temperature in the room becomes 18 °C.

Figure 8 shows the T_{pv} , condenser temperature (T_{con}), and room temperature (T_{room}) when hot water, PV cooling, and space cooling were delivered simultaneously. During the experimentation, the average T_{pv} , T_{con} , and T_{room} were found to be 34.59 °C, 46.27 °C, and 23.35 °C. The maximum temperature of condenser water was recorded as 60.32 °C at 14:00. The maximum and minimum room temperatures were 26.55 °C and 18.37 °C, respectively, during the day. Except from 11:00 to 13:00, the room is constantly kept below 28 °C, as indicated in Figure 8. However, the proposed system effectively cooled the room and PV panel and heated the water for building needs.

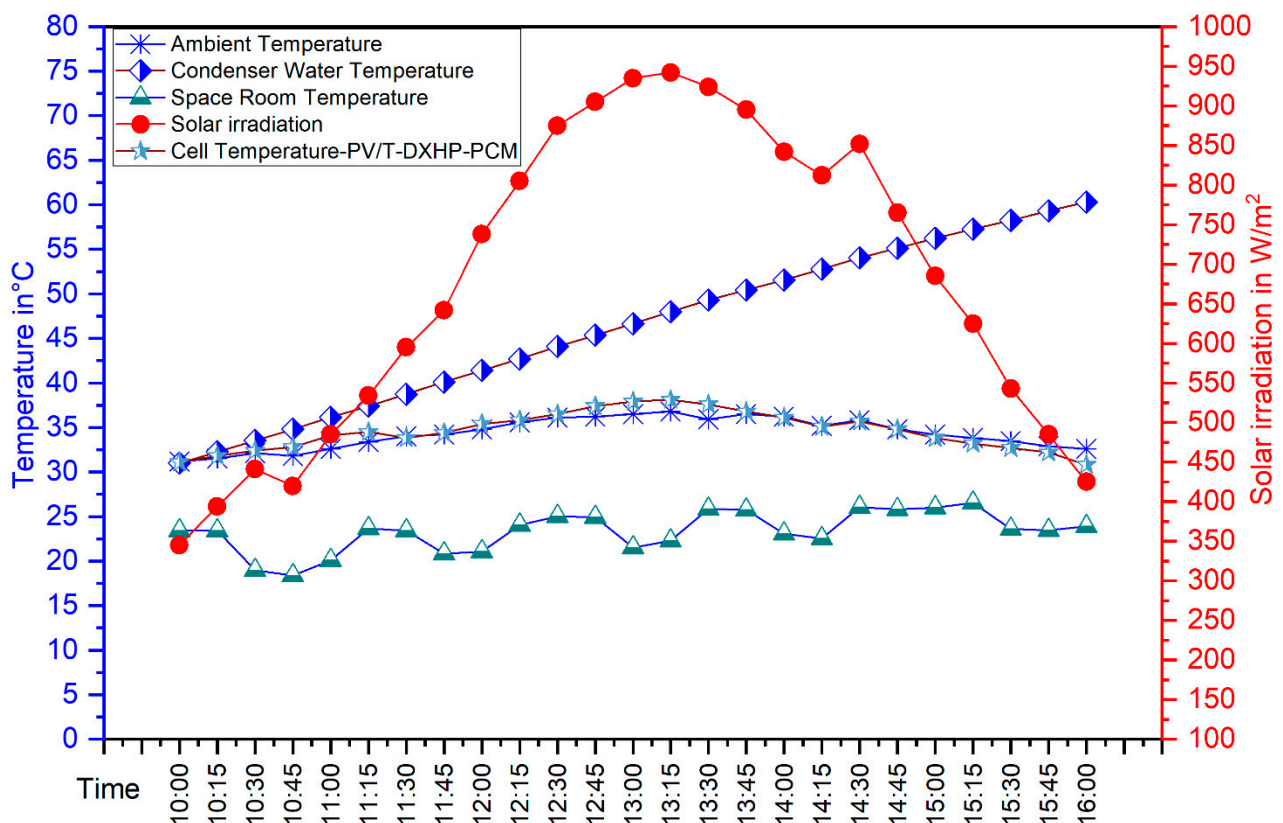


Figure 8. Hourly variation of T_{pv} , T_{con} , and T_{room} .

Figure 9 depicts the hourly variation of a proposed system's COP_{HP} , $COP_{overall}$, Q_e , and Q_c . On average, the condenser can hold a temperature range of 3335 W at 11:30 and 2294 W at 14:00. Similarly, the amount retrieved from the room was 1380 W and 2873 W, respectively. The heat pump's COP varied from 5.89 to 2.36, with 4.15 being the average value. The hybrid PV/T-DXHP-PCM system was operated in a wide range of typical outside ambient temperatures and the average overall COP of the proposed system was

5.51 in this field test. According to this research, the average useful thermal energy that heat pump systems produced was 2.89 kW. Assuming the heat pump’s power is constant, the system’s COP should theoretically improve when the heat exchange energy in the evaporator and the water heating activity is high. However, the increase in T_{con} is causing the consumption of electrical energy by the compressor to continue its upward trend. A total energy of 4.73 kWh was consumed by the PV/T-DXHP-PCM system up of a fan, solenoid valve, and a compressor. The findings indicate that the overall COP for the HP system falls somewhere in the range of 2.82 to 9.33. This range was determined, when water heating, change in PV/T power, and space cooling were achieved by supplying electricity. It is essential to keep in mind that the coefficients of performance (COPs) can range from one system to another because each heat pump has its own unique configuration, heating intensity, climate conditions, design, and control strategy.

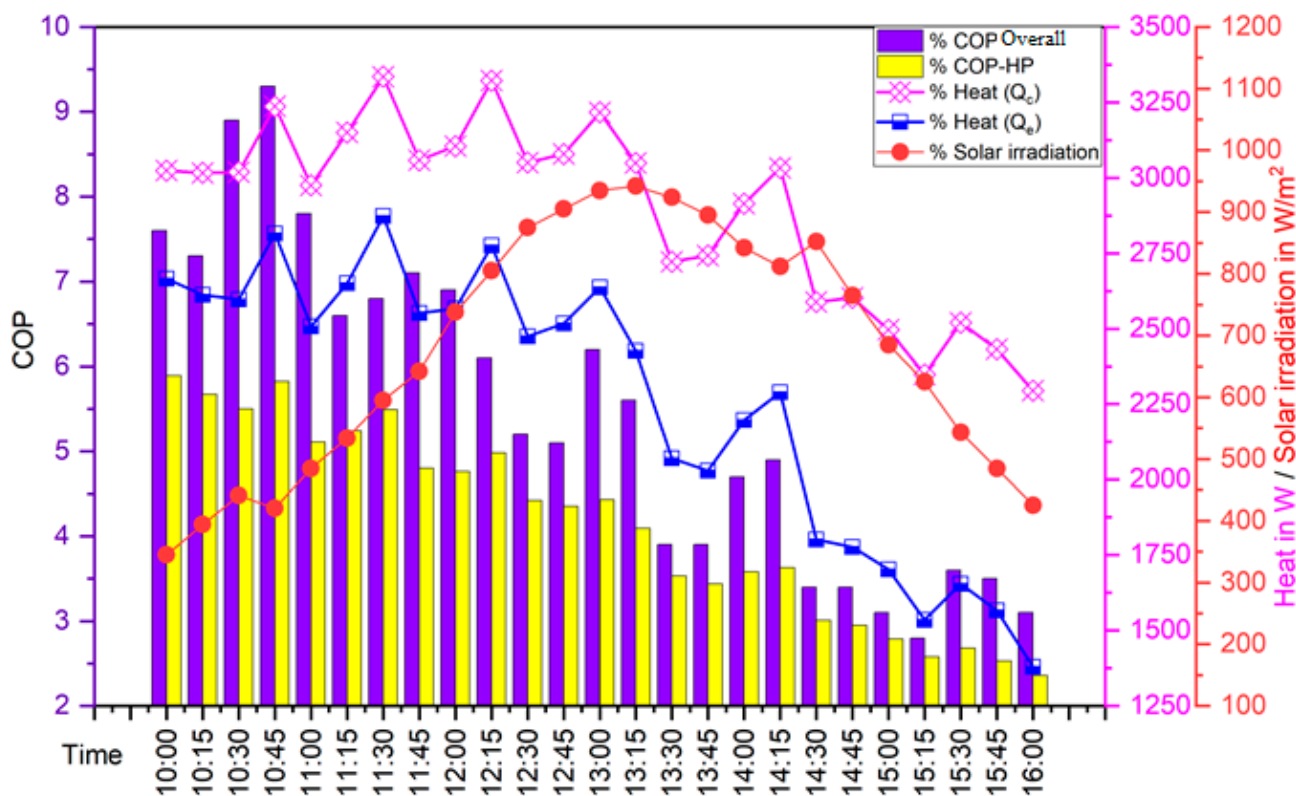


Figure 9. Hourly variation of COP_{HP}, COP_{Overall}, Q_e, and Q_c.

It was observed that the simultaneous heat removal carried out by the PV/T-PCM and ASE evaporator, the condenser, and the COP were inversely proportional to the water temperature when the condenser water temperature rose from 30 °C to 60 °C. Also, it has been seen that as the temperature of the condenser water goes up, the pressure inside the condenser goes up as well. As the temperature of the condenser water rises, it can be seen that both the heat capacities and the COP fall to lower values. This is because the condenser cannot release heat when the water temperature is high because it cannot exchange heat. No matter what method was used, the COP of the system goes down a lot as T_c goes up compared to the other modes of operation. As the amount of solar irradiation increases, so do the heat capacities and the pressures of condensation and evaporation. This is because increased solar irradiation makes it possible for the PV/T evaporator to exchange more heat energy instantly. So, high solar irradiation levels lead to a higher refrigerant mass flow rate and high temperatures and pressures in the evaporator. All of these things improve the performance of the system.

Figure 10 indicates the total heat removed by the refrigerant from the PCM (charging) and the full heat taken by the PV/T system (discharging) during an experimentation day. By 10:30, the PCM had fully charged, and the refrigerant had stopped flowing into the PV/T-PCM evaporator system. The heat stored by the PCM was used to cool and maintain the temperature of the PV/T system. The PCM discharges its stored heat to the PV panel within 11:00, and refrigerant flows into the PV/T-PCM evaporator. It followed a similar trend during the remaining period but took only 30 min to discharge. When solar radiation was low, it took more time (45 min) to discharge during the evening and morning. The COP and Q_e were high during the PCM discharging period as more refrigerant entered into the air source evaporator. As a result, it is reasonable to infer that using refrigerant and PCM cools the PV panel, increasing the panel's efficiency and electrical output.

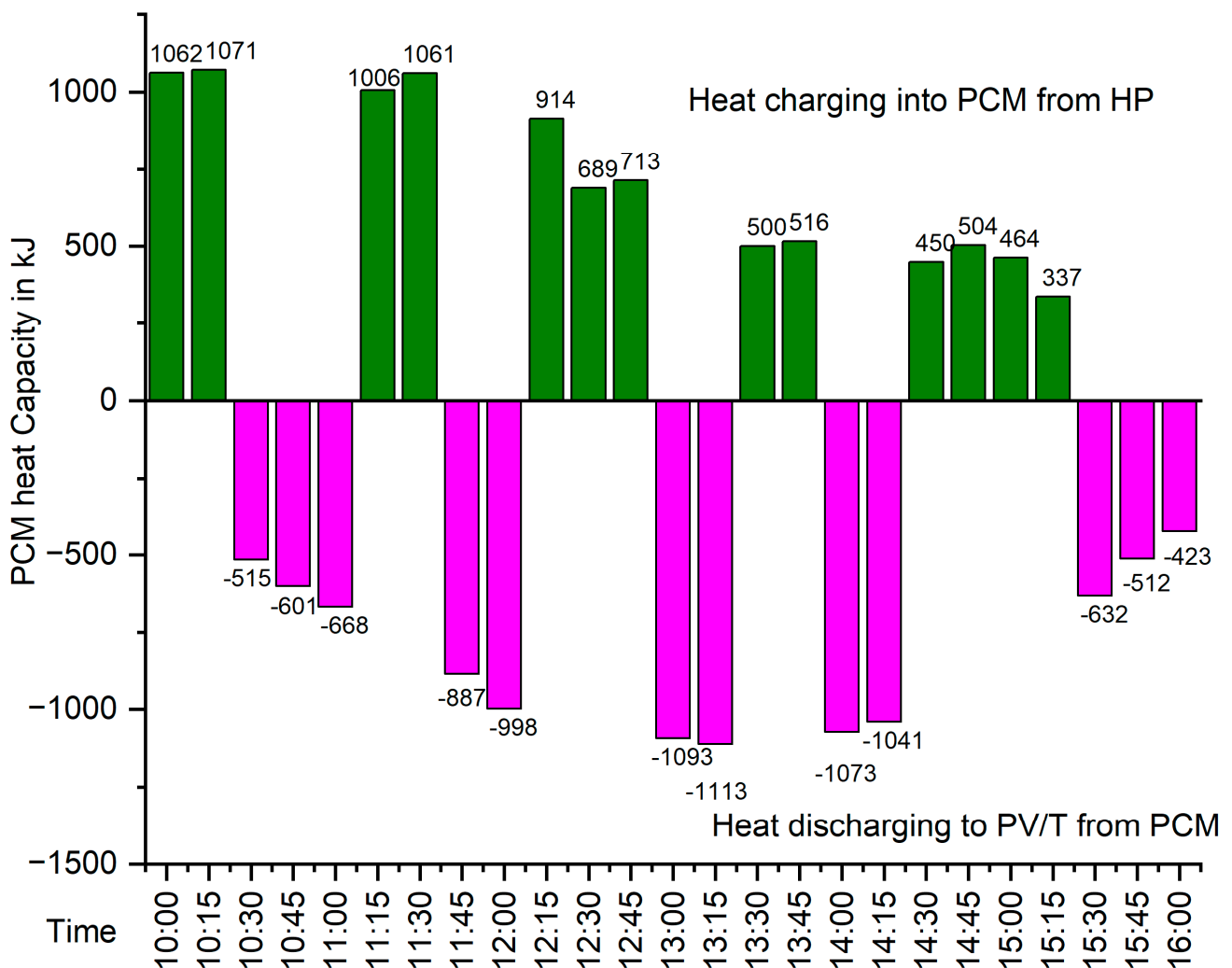


Figure 10. Hourly variation of PCM Charging and discharging capacity.

As a result, the impact of cooling can be effective even at higher radiation levels, which results in the best possible electrical efficiency. In addition, the refrigeration effect causes the sink temperature (P/V panel) to be inverted in the PV/T-DXHP-PCM system. As a result, there was a significant improvement in the effectiveness of the heat degradation PV module. However, the observed temperature fluctuations indicate that there was an irregularity in the heat diffusion potential across the encapsulation. Meanwhile, the HS36 PCM contribution allowed for some sustained temperature decline, which aids in maintaining a steady PV module temperature despite the anomalous radiation decrease that was experienced. Overall, the proposed PV/T-DXHP-PCM installation has kept the

room space temperature at a human comfort level, cooled the PV panel, and heated the 600 litres of water by consuming 4.64 kWh of energy per day. Hence, these systems fulfilled the building requirements. Furthermore, if the refrigerant supplied by the heat pump can provide a lower temperature than the previous output, the PV/T temperature remains reduced. More research is required to examine enhancements and optimization possibilities to acquire maximum performance from the proposed hybrid PV/T-DXHP-PCM system.

3.3. Comparison of Performance of the Present Study with the Previous Study

Table 5 displays the results of a comparison between the suggested PV/T-DXHP-PCM system and the existing literature on the subject. The results of PV/T-DXHP-PCM were found to be either vastly superior to or on par with those of other published methods.

Table 5. Comparing the present study with the available literature.

Reference Paper	Electrical Efficiency in %	Thermal Efficiency in %	COP
[37]	10.4	49.3	4.1
[38]	14.5	51.5	4.08
[39]	12.1	57.5	3.66
[34]	7.51	49.9	3.45
[40]	15	65	6.4
Present Study	14.14	104.38	5.51

4. Conclusions and Future Scope of Work

This work investigated the performance of a hybrid PV/T DXHP system with PCM in India by measuring its ability to produce hot water (at 60 °C), space cooling (below 26 °C), and electricity. A hybrid PV/T heat pump with PCM was operated under the dynamic conditions of a day, and its suitability for buildings was assessed. Its findings are as follows:

1. The innovative hybrid PV/T-DXHP-PCM technology enhanced both the PV/T module and the heat pump's electrical and thermal performance. The heat from the PV/Ts not only increased the heat pump's ability to cool, but it also increased the amount of heat needed to heat the water.
2. The system's average electrical efficiency of 14.14% was achieved, which was near the PV panel's STC. The PV/T system's electrical efficiency was 47.91% higher than the standard PV system.
3. The average thermal efficiency of the proposed system was 104.38%. The overall efficiency of the system was 117.58%. The system's heating and cooling COP were recorded as 5.51 and 4.62.
4. The hybrid PV/T-DXHP-PCM system effectively generated the hot water and space cooling needs along with electricity generation, which avoided using the individual system for water heating, space cooling, and power generation.
5. In terms of thermal and electrical efficiency, the PVT system demonstrates very high values. As one of the largest energy consumers among public buildings, hospitals can significantly benefit from increased energy output to reduce their annual operating costs. However, more research needs to be performed to figure out how to improve hybrid systems to achieve the best production. As an illustration, future optimization work may increase the heat pump's COP.

Author Contributions: Conceptualization, M.K.P.; Methodology, K.B.P. and S.C.; Validation, M.A.; Formal analysis, K.B.P. and M.A.; Investigation, K.B.P.; Resources, M.A. and S.S.; Data curation, S.S.; Writing—original draft, K.B.P.; Writing—review & editing, S.C. and S.R.R.; Supervision, M.K.P.; Project administration, M.K.P.; Funding acquisition, M.K.P. All authors have read and agreed to the published version of the manuscript.

Funding: This research received no external funding.

Data Availability Statement: The data supporting the findings of this study are available within the article.

Conflicts of Interest: The authors declare no conflict of interest.

Nomenclature

Symbol	Description
PV	Photovoltaic System
PV/T	Photovoltaic thermal System
HP	Heat pump
PCM	Phase change materials
SC	Space Cooling
WH	Water heating
H/C	Heating and cooling
LH	Latent Heat
COP	Coefficient of Performance
DX	Direct Expansion
IX	Indirect Expansion
CC	Cooling Capacity
P	Power
V_{mp} at P_{max}	Voltage at Pmax
I_{mp} at P_{max}	Current at Pmax
V_{oc}	Open Circuit Voltage
I_{sc}	Short Circuit Current
T_m	Melting Temperature
T_f	Freezing Temperature
Q_{lh}	Latent Heat
ρ_l	Density at liquid state
ρ_s	Density at solid state
C_{pl}	Specific Heat at liquid state
C_{ps}	Specific Heat at solid state
K_l	Thermal Conductivity at liquid state
K_s	Thermal Conductivity at solid state
C	Specific heat
Q	Heat
max	maximum
min	Minimum
c	Condenser
e	Evaporator
W	Water
T	Temperature
η	Efficiency
el	Electrical
th	Thermal
V	Volume
E	Power
r	Rated
I	Current
R	Refrigerant
CT	Capillary Tube
OD	Outer diameter
ID	Inner Diameter

References

1. Pathak, H. Impact, Adaptation, and Mitigation of Climate Change in Indian Agriculture. *Environ. Monit. Assess.* **2023**, *195*, 52. [[CrossRef](#)] [[PubMed](#)]
2. Ramya, D.; Krishnakumari, A.; Dineshkumar, P.T.; Srivastava, M.P.; Kannan, L.V.; Puthilibai, G.; Kumar, P.M. Investigating the influence of nanoparticle disbanded phase changing material (NDPCM) on the working of solar PV. *Mater. Today Proc.* **2022**, *56*, 1341–1346. [[CrossRef](#)]
3. Akadiri, S.S.; Adebayo, T.S. Asymmetric Nexus among Financial Globalization, Non-Renewable Energy, Renewable Energy Use, Economic Growth, and Carbon Emissions: Impact on Environmental Sustainability Targets in India. *Environ. Sci. Pollut. Res.* **2022**, *29*, 16311–16323. [[CrossRef](#)] [[PubMed](#)]
4. Barone, G.; Buonomano, A.; Faninger, G.; Forzano, C.; Giuzio, G.F.; Kalogirou, S.A.; Palombo, A. Solar Hot Water Heating Systems. In *Comprehensive Renewable Energy*; Elsevier: Amsterdam, The Netherlands, 2022; pp. 463–500.
5. Alharbi, F.H.; Kais, S. Theoretical Limits of Photovoltaics Efficiency and Possible Improvements by Intuitive Approaches Learned from Photosynthesis and Quantum Coherence. *Renew. Sustain. Energy Rev.* **2015**, *43*, 1073–1089. [[CrossRef](#)]
6. Baus, L.; Nehr, S. Potentials and Limitations of Direct Air Capturing in the Built Environment. *Build. Environ.* **2022**, *208*, 108629. [[CrossRef](#)]
7. Fischer, D.; Madani, H. On Heat Pumps in Smart Grids: A Review. *Renew. Sustain. Energy Rev.* **2017**, *70*, 342–357. [[CrossRef](#)]
8. Khouya, A. Performance Assessment of a Heat Pump and a Concentrated Photovoltaic Thermal System during the Wood Drying Process. *Appl. Therm. Eng.* **2020**, *180*, 115923. [[CrossRef](#)]
9. Khouya, A. Levelized Costs of Energy and Hydrogen of Wind Farms and Concentrated Photovoltaic Thermal Systems. A Case Study in Morocco. *Int. J. Hydrogen Energy* **2020**, *45*, 31632–31650. [[CrossRef](#)]
10. Kamel, R.S.; Fung, A.S.; Dash, P.R.H. Solar Systems and Their Integration with Heat Pumps: A Review. *Energy Build.* **2015**, *87*, 395–412. [[CrossRef](#)]
11. Ahmadi, S.; Sheikh-Zeinoddin, M.; Soleimani-Zad, S.; Alihosseini, F.; Yadav, H. Effects of Different Drying Methods on the Physicochemical Properties and Antioxidant Activities of Isolated Acorn Polysaccharides. *LWT* **2019**, *100*, 1–9. [[CrossRef](#)]
12. Lin, Y.; Bu, Z.; Yang, W.; Zhang, H.; Francis, V.; Li, C.-Q. A Review on the Research and Development of Solar-Assisted Heat Pump for Buildings in China. *Buildings* **2022**, *12*, 1435. [[CrossRef](#)]
13. Kong, R.; Deethayat, T.; Asanakham, A.; Kiatsiriroat, T. Performance and Economic Evaluation of a Photovoltaic/Thermal (PV/T)-Cascade Heat Pump for Combined Cooling, Heat and Power in Tropical Climate Area. *J. Energy Storage* **2020**, *30*, 101507. [[CrossRef](#)]
14. Besagni, G.; Croci, L.; Nesa, R.; Molinaroli, L. Field Study of a Novel Solar-Assisted Dual-Source Multifunctional Heat Pump. *Renew. Energy* **2019**, *132*, 1185–1215. [[CrossRef](#)]
15. Shao, N.; Ma, L.; Zhang, J. Experimental Investigation on the Performance of Direct-Expansion Roof-PV/T Heat Pump System. *Energy* **2020**, *195*, 116959. [[CrossRef](#)]
16. Li, H.; Sun, Y. Operational Performance Study on a Photovoltaic Loop Heat Pipe/Solar Assisted Heat Pump Water Heating System. *Energy Build.* **2018**, *158*, 861–872. [[CrossRef](#)]
17. Zhou, J.; Zhu, Z.; Zhao, X.; Yuan, Y.; Fan, Y.; Myers, S. Theoretical and Experimental Study of a Novel Solar Indirect-Expansion Heat Pump System Employing Mini Channel PV/T and Thermal Panels. *Renew. Energy* **2020**, *151*, 674–686. [[CrossRef](#)]
18. Yu, M.; Chen, F.; Zheng, S.; Zhou, J.; Zhao, X.; Wang, Z.; Li, G.; Li, J.; Fan, Y.; Ji, J.; et al. Experimental Investigation of a Novel Solar Micro-Channel Loop-Heat-Pipe Photovoltaic/Thermal (MC-LHP-PV/T) System for Heat and Power Generation. *Appl. Energy* **2019**, *256*, 113929. [[CrossRef](#)]
19. Song, Z.; Ji, J.; Li, Z. Comparison Analyses of Three Photovoltaic Solar-Assisted Heat Pumps Based on Different Concentrators. *Energy Build.* **2021**, *251*, 111348. [[CrossRef](#)]
20. Bisengimana, E.; Zhou, J.; Binama, M.; Yuan, Y. Numerical Investigation on the Factors Influencing the Temperature Distribution of Photovoltaic/Thermal (PVT) Evaporator/Condenser for Heat Pump Systems. *Renew. Energy* **2022**, *194*, 885–901. [[CrossRef](#)]
21. Abbas, S.; Yuan, Y.; Hassan, A.; Zhou, J.; Zeng, C.; Yu, M.; Emmanuel, B. Experimental and Numerical Investigation on a Solar Direct-Expansion Heat Pump System Employing PV/T & Solar Thermal Collector as Evaporator. *Energy* **2022**, *254*, 124312. [[CrossRef](#)]
22. Sarikarin, T.; Suksri, A.; Wongwuttanasatian, T. Temperature Compensation of Photovoltaic Cell Using Phase Change Materials. *Int. J. Eng. Technol.* **2018**, *7*, 179. [[CrossRef](#)]
23. Sarikarin, T.; Wongwuttanasatian, T.; Suksri, A. Cooling Enhancement of Photovoltaic Cell via the Use of Phase Change Materials in a Different Designed Container Shape. *IOP Conf. Ser. Earth Environ. Sci.* **2019**, *257*, 012046. [[CrossRef](#)]
24. Velmurugan, K.; Karthikeyan, V.; Korukonda, T.B.; Poongavanam, P.; Nadarajan, S.; Kumarasamy, S.; Wongwuttanasatian, T.; Sandeep, D. Experimental Studies on Photovoltaic Module Temperature Reduction Using Eutectic Cold Phase Change Material. *Sol. Energy* **2020**, *209*, 302–315. [[CrossRef](#)]
25. Al-Omari, S.A.B.; Qureshi, Z.A.; Elnajjar, E.; Mahmoud, F. A Heat Sink Integrating Fins within High Thermal Conductivity Phase Change Material to Cool High Heat-Flux Heat Sources. *Int. J. Therm. Sci.* **2022**, *172*, 107190. [[CrossRef](#)]
26. Al-Omari, S.A.B.; Qureshi, Z.A.; Mahmoud, F.; Elnajjar, E. Thermal Management Characteristics of a Counter-Intuitive Finned Heat Sink Incorporating Detached Fins Impregnated with a High Thermal Conductivity-Low Melting Point PCM. *Int. J. Therm. Sci.* **2022**, *175*, 107396. [[CrossRef](#)]
27. Qureshi, Z.A.; Al-Omari, S.A.B.; Elnajjar, E.; Al-Ketan, O.; Abu Al-Rub, R. Nature-Inspired Triply Periodic Minimal Surface-Based Structures in Sheet and Solid Configurations for Performance Enhancement of a Low-Thermal-Conductivity Phase-Change Material for Latent-Heat Thermal-Energy-Storage Applications. *Int. J. Therm. Sci.* **2022**, *173*, 107361. [[CrossRef](#)]

28. Qureshi, Z.A.; Elnajjar, E.; Al-Ketan, O.; Al-Rub, R.A.; Al-Omari, S.B. Heat Transfer Performance of a Finned Metal Foam-Phase Change Material (FMF-PCM) System Incorporating Triply Periodic Minimal Surfaces (TPMS). *Int. J. Heat Mass Transf.* **2021**, *170*, 121001. [[CrossRef](#)]
29. Velmurugan, K.; Kumarasamy, S.; Wongwuttanasatian, T.; Seithtanabutara, V. Review of PCM Types and Suggestions for an Applicable Cascaded PCM for Passive PV Module Cooling under Tropical Climate Conditions. *J. Clean. Prod.* **2021**, *293*, 126065. [[CrossRef](#)]
30. Calabrò, E. An Algorithm to Determine the Optimum Tilt Angle of a Solar Panel from Global Horizontal Solar Radiation. *J. Renew. Energy* **2013**, *2013*, 307547. [[CrossRef](#)]
31. Hossain, M.S.; Pandey, A.K.; Selvaraj, J.; Abd Rahim, N.; Rivai, A.; Tyagi, V.V. Thermal Performance Analysis of Parallel Serpentine Flow Based Photovoltaic/Thermal (PV/T) System under Composite Climate of Malaysia. *Appl. Therm. Eng.* **2019**, *153*, 861–871. [[CrossRef](#)]
32. Hossain, M.S.; Pandey, A.K.; Selvaraj, J.; Rahim, N.A.; Islam, M.M.; Tyagi, V.V. Two Side Serpentine Flow Based Photovoltaic-Thermal-Phase Change Materials (PVT-PCM) System: Energy, Exergy and Economic Analysis. *Renew. Energy* **2019**, *136*, 1320–1336. [[CrossRef](#)]
33. Long, T.; Qiao, Z.; Wang, M.; Li, Y.; Lu, J.; Li, W.; Zeng, L.; Huang, S. Performance Analysis and Optimization of a Solar-Air Source Heat Pump Heating System in Tibet, China. *Energy Build.* **2020**, *220*, 110084. [[CrossRef](#)]
34. Lu, S.; Liang, R.; Zhang, J.; Zhou, C. Performance Improvement of Solar Photovoltaic/Thermal Heat Pump System in Winter by Employing Vapor Injection Cycle. *Appl. Therm. Eng.* **2019**, *155*, 135–146. [[CrossRef](#)]
35. Zhou, C.; Liang, R.; Zhang, J.; Riaz, A. Experimental Study on the Cogeneration Performance of Roll-Bond-PVT Heat Pump System with Single Stage Compression during Summer. *Appl. Therm. Eng.* **2019**, *149*, 249–261. [[CrossRef](#)]
36. Elminshawy, A.; Morad, K.; Elminshawy, N.A.S.; Elhenawy, Y. Performance Enhancement of Concentrator Photovoltaic Systems Using Nanofluids. *Int. J. Energy Res.* **2021**, *45*, 2959–2979. [[CrossRef](#)]
37. Bai, Y.; Chow, T.T.; Ménézo, C.; Dupeyrat, P. Analysis of a Hybrid PV/Thermal Solar-Assisted Heat Pump System for Sports Center Water Heating Application. *Int. J. Photoenergy* **2012**, *2012*, 265838. [[CrossRef](#)]
38. Wang, G.; Quan, Z.; Zhao, Y.; Sun, C.; Deng, Y.; Tong, J. Experimental Study on a Novel PV/T Air Dual-Heat-Source Composite Heat Pump Hot Water System. *Energy Build.* **2015**, *108*, 175–184. [[CrossRef](#)]
39. Zhang, T.; Pei, G.; Zhu, Q.; Ji, J. Experimental Study of a Novel Photovoltaic Solar-Assisted Heat Pump/Loop Heat-Pipe (PV-SAHP/LHP) System. *IOP Conf. Ser. Earth Environ. Sci.* **2017**, *52*, 012017. [[CrossRef](#)]
40. James, A.; Srinivas, M.; Mohanraj, M.; Raj, A.K.; Jayaraj, S. Experimental Studies on Photovoltaic-Thermal Heat Pump Water Heaters Using Variable Frequency Drive Compressors. *Sustain. Energy Technol. Assess.* **2021**, *45*, 101152. [[CrossRef](#)]

Disclaimer/Publisher’s Note: The statements, opinions and data contained in all publications are solely those of the individual author(s) and contributor(s) and not of MDPI and/or the editor(s). MDPI and/or the editor(s) disclaim responsibility for any injury to people or property resulting from any ideas, methods, instructions or products referred to in the content.